2019 International Symposium on Nonlinear Theory and Its Applications
NOLTA2019, Kuala Lumpur, Malaysia, December 2-6, 2019.

Analysis of Phase-Inversion Waves and Phase-Waves by Instantaneous Expanding Rates

Rika Hirano†, Masayuki Yamauchi†, and Yoshifumi Nishio‡

†Dept. of Elec. and Comp. Eng., Hiroshima Institute of Technology, 2-1-1 Miyake, Saeki-ku, Hiroshima 731-5193, Japan
‡Dept. of Elec. and Elec. Eng., Tokushima University, 2-1 MinamiJyosanjima-cho, Tokushima 770-8506, Japan
Email: ma19017@cc.it-hiroshima.ac.jp

Abstract—In this paper, we define an instantaneous expanding rate which is defined as a change rate of value of voltage on Poincare section of which a current is zero in each oscillator. Furthermore, we define an quasi Lyapunov exponent. We observe and analyze the phase-inversion waves and the phase-waves by using the instantaneous expanding rates and the quasi Lyapunov exponents.

1. Introduction

Various things and living are synchronizing and resonating in this natural world[1]. The phenomena are built by the oscillation phenomena, and two things can synchronize when the two things have almost same natural frequency and oscillators can affect each other even if distance between the two things is far. Therefore, the synchronization phenomena are critically needed to the communication systems. Furthermore, the synchronization phenomena are very close phenomenon to living things and one of essential phenomena for people living. For instance, in south-east Asia, it is observed that blink of a large number of fireflies on a tree synchronize. It is considered important to observe and to analyze such synchronization phenomena in order to know and use various phenomena in this natural world.

In our previous study, we have been observing and analyzing the synchronization phenomen on the coupled oscillators systems which are ring, ladder and 2D lattice shapes. We discovered a propagating wave which is continuously switching phase states between two adjacent oscillators on the ladder from in-phase synchronization to anti-phase synchronization or anti-phase synchronization to in-phase synchronization[2]. We named this phenomenon a phase-inversion wave. The phase-inversion waves can be observed on the van der Pol oscillators coupled as the ladder, the ring, the 2D lattice, and so on, when nonlinearity is weak. We discovered another wave which disappears or becomes phase-inversion waves in propagating[3]. The phenomenon is named phase-waves. We have been investigating and analyzing the phase-inversion waves and the phase-waves by using instantaneous electric power of each oscillator, instantaneous frequencies, and phase differences between adjacent oscillators. The phase-waves are hard to distinguished for phase-inversion waves in short time, and the phase-waves are hard to observe when the phase-waves is propagating small phase difference. Differences in each phenomenon have been confirmed using the instantaneous electric powers. However, minutia difference between phase-waves and phase-inversion waves was not enough analyzed. The phase-waves which is propagating small phase differences are hard to observe, but it is guessed that the small phase-waves affect other wave phenomena. Therefore, the small phase-waves have to be investigated and analyzed

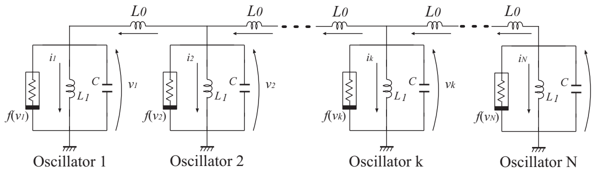

Figure 1: Circuit model.

In this study, we define as an instantaneous expanding rate (IER) a change rate of a value of voltage on Poincare section of which a current is zero in each oscillator, and a quasi Lyapunov exponent (QLE) is defined by using behavior of the voltage on the Poincare section. We suggest to investigate and to analyze by using the IER and the QLE. The phase-inversion waves and phase-waves are observed by using the IER and the QLE on the ladder of van der Pol oscillators. The phase-waves propagating small phase difference are observed.

2. Circuit Model

Our circuit model, which N van der Pol oscillators are coupled by inductors as a ladder, are shown in Fig.1. Each van der Pol oscillator is called OSC_k:$(1 \le k \le N)$. An inductor and a capacitor of each van der Pol oscillator are shown as L_1 and C, respectively. A voltage of OSC_k is expressed as v_k and an electric current in L_1 is expressed as i_k. A non-linear negative resistor is expressed as Eq. (1).

$$f(v_k) = -g_1 v_k + g_3 v_k^3 \quad (g_1,\ g_3 > 0) \tag{1}$$

<Normalized Circuit Equation>

Circuit equations are normalized by Eq.(2). The normalized equations are shown in Eqs. (3)–(5).

$$\begin{aligned} i_{L_1} &= \sqrt{\frac{Cg_1}{3L_1 g_3}}x_k,\ \ v_k = \sqrt{\frac{g_1}{3g_3}}y_k, t = \sqrt{L_1 C}\tau, \\ \alpha &= \frac{L_1}{L_0},\ \ \varepsilon = g_1\sqrt{\frac{L_1}{C}},\ \ \frac{d}{d\tau} = \text{“ · ”},\ \ \delta = \frac{g_1^2}{3g_3}. \end{aligned} \tag{2}$$

<1_{st} Oscillator ($k = 1$)>

$$\begin{aligned} \dot{x}_k &= y_k, \\ \dot{y}_k &= -x_k + \alpha(x_{k+1} - x_k) + \varepsilon(y_k - \frac{1}{3}y_k^3). \end{aligned} \tag{3}$$

<Middle Oscillators ($1 < k < N$)>

$$\begin{aligned} \dot{x}_k &= y_k, \\ \dot{y}_k &= -x_k + \alpha(x_{k+1} - 2x_k + x_{k-1}) + \varepsilon(y_k - \frac{1}{3}y_k^3). \end{aligned} \tag{4}$$

<N_{th} Oscillator ($k = N$)>

$$\dot{x}_k = y_k,$$
$$\dot{y}_k = -x_k + \alpha(x_{k-1} - x_k) + \varepsilon(y_k - \frac{1}{3}y_k^3), \quad (5)$$

where α is strength of coupling, and ε expresses strength of non-linearity. We analyze these circuit equations by the fourth Runge-Kutta method. We fix stepsize of Runge-Kutta method is 0.001 in this study.

3. Instantaneous Expanding Rate and Quasi Lyapunov exponent

We obtain a Poincare section, and an instantaneous expanding rate (IER) and a quasi Lyapunov exponent (QLE) are defined by using numerical simulations.

3.1. Poincare section

We calculate y_k on Poincare section of when x_k is zero. We assume l-th calculation results are $x_k(l)$ and $y_k(l)$, and the time is assumed as $\tau(l)$. $(l+1)$-th calculation results express $x_k(l+1)$ and $y_k(l+1)$, and the time expresses $\tau(l+1)$. We assume the $x_k(l)$ is larger than 0, and the $x_k(l+1)$ is smaller than 0. A value of y_k on Poincare section is calculated by Eq. (6). The value is shown as $yp_k(l)$.

$$yp_k(l) = y_k(l) + sign \cdot \frac{x_k(l) \cdot |y_k(l+1) - y_k(l)|}{x_k(l) - x_k(l+1)}. \quad (6)$$

{If $y_k(l+1) \geq y_k(l)$, $sign = 1$. If $y_k(l+1) < y_k(l)$, $sign = -1$.}

The time $\tau p_k(l)$ of $yp_k(l)$ is assumed by Eq. (7).

$$\tau p_k(l) = \tau_k(l) + \frac{x_k(l) \cdot (\tau_k(l+1) - \tau_k(l))}{x_k(l) - x_k(l+1)}. \quad (7)$$

3.2. Instantaneous expanding rate (*IER*)

The l-th time value on Poincare section is shown as $yp_k(l)$, and the value of $(l+1)$-th time is expressed as $yp_k(l+1)$. The *IER* is defined as Eq.(8).

$$IER(l) = \frac{yp_k(l+1) - yp_k(l)}{yp_k(l)}. \quad (8)$$

3.3. Quasi Lyapunov exponent (*QLE*)

In this paper, below value is called quasi Lyapunov exponent, because *QLE* is calculated by considering only x_k and y_k in OSC_k without other oscillators. The *QLE* is calculated by Eq.(9).

$$QLE = \frac{1}{m}\sum_{l=1}^{m} \ln\left|\frac{yp_k(l+1) - yp_k(l)}{\tau p_k(l+1) - \tau p_k(l)}\right|. \quad (9)$$

4. Phase-Inversion Waves and Phase-Waves

The *IER*s and the *QLE*s of the phase-inversion waves and the phase-waves are investigated. The observation conditions are set as follows.

1. N is fixed 200.
2. Strength of the non-linearity ε, and strength of the coupling α are fixed as 0.3 and 0.05, respectively.
3. Maximum calculation time is 483000τ.
4. We observe two type phase-inversion waves. First type is that time between first and second phase-inversion waves is very short. Second type is that the time between first and second phase-inversion waves is around 650τ. We call the two type as thin-type phase-inversion waves and wide-type phase-inversion waves, respectively.

When the synchronization states are in-phase, the *QLE* is around -18.15. The *QLE* is around -17.87 when anti-phase synchronization is observed. We can guess that *QLE* is minus infinity in theory, but *QLE*s are obtained above values because numerical simulation is used.

4.1. Wide-type phase-inversion waves

<Phase state>

Figure 2(a) shows itinerancies of phase states between adjacent oscillators from 0τ to 16100τ. The Fig. 2(a) shows two hundred horizontally long slim boxes which are piled up vertically. Horizontal axis of each slim box expresses time. Vertical axis of each slim box expresses a sum of voltages of adjacent oscillators. For instance, the top slim box shows an itinerancy of phase state between OSC_0 and OSC_1 along time. The next slim box shows an itinerancy of phase state between OSC_1 and OSC_2 along time. The bottom slim box shows an itinerancy of phase state between OSC_{198} and OSC_{199} along time. A vibration is large in the slim box, when a phase states between adjacent oscillators is in-phase synchronization. When the phase state between adjacent oscillators is the anti-phase synchronization, the vibration decreases to zero. Therefore, black regions show near in-phase synchronization and white regions show near anti-phase synchronization. We can understand that the second phase-inversion wave, which changes from anti-phase synchronization to in-phase synchronization, propagate after the first phase-inversion wave, which changes from in-phase synchronization to anti-phase synchronization, propagates. The time between first and second phase-inversion waves is almost 650τ.

<Instantaneous expanding rate>

Figures 2(b)-(e) show the result of *IER*s. Vertical axis expresses *IER*. Horizontal axis expresses time. Itinerancies of *IER*s are piled up and shown in the Figs. 2(b) and (c). Top line expresses itinerancy of IER_0 of OSC_0 bottom graph expresses IER_{199} of OSC_{199}. The Fig. 2(b) shows itinerancies of *IER*s during 483000τ. The Fig. 2(c) is extended figure of the Fig. 2(b) from 0τ to 16100τ. Figures 2(d) and (e) shows extended figures of a yellow rectangle box of the Fig. 2(c). The Fig. 2(d) shows behavior of IER_{50} of when a phase state is changed from in-phase synchronization to anti-phase synchronization by the first phase-inversion wave. The Fig. 2(e) shows behavior of IER_{50} of when a phase state is changed from anti-phase synchronization to in-phase synchronization by the second phase-inversion wave. When a phase-inversion wave propagates, IER_{50} slightly increase, decrease, increase and become zero again. In other words, two peaks for positive values and one peak for negative value can be observed, when a phase state is switched in-phase and anti-phase.

<Quasi Lyapunov exponent>

Figure 2(f) shows QLE_{50}. Vertical axis expresses *QLE*. Horizontal axis is time. *QLE* asymptotically becomes to around -13.

4.2. Thin-type phase-inversion waves

<Phase state>

Figure 3(a) shows itinerancies of phase states between adjacent oscillators from 0τ to 16100τ. We can observe the thin-type phase-inversion waves.

<Instantaneous expanding rate>

Figures 3(b)-(d) show the IERs. The Fig. 3(b) shows itinerancies of IERs from 0τ to 483000τ. The Fig. 3(c) shows a extended figure of yellow box of the Fig. 3(b). The Fig. 3(d) shows a extended figure of yellow box of the Fig. 3(c). The Fig. 3(d) shows itinerancy of IER_{50} from 11431τ to 11914τ. We can observed three peaks of positive values and two peaks of negative values in the Fig. 3(d). We can understand that second peak of positive value by first phase-inversion wave is combined first peak of positive value by second phase-inversion wave, because time between the first and the second phase-inversion waves is very short.

<Quasi Lyapunov exponent>

Figure 3(e) shows QLE_{50}. The Fig. 3(e) is similar to the Fig. 2(f). QLE asymptotically becomes to around -13.

4.3. Phase-waves

<Phase state>

Figure 4(a) shows itinerancies of phase states from 0τ to 16100τ. Details of phase-waves are hard to observe on this figure.

<Instantaneous expanding rate>

Figures 4(b), and (c) show the IERs. The Fig. 4(b) shows all itinerancies of IERs. The Fig. 4(c) shows a extended figure of yellow box of the Fig. 4(b). A range of vertical axis of the Fig. 4(c) is almost 0.01 times of the Figs. 2(d) and 3(d). We can understand that fluctuation is very small, and form of behavior in Fig. 4(c) differs forms of behaviors in the Figs. 2(d) and 3(d). There are two peaks of positive values and two peaks of negative values. Furthermore, the phase-waves in the Fig. 2(a) is hard to observe, but the phase-waves in the Fig. 2(b) is shown clear. We can understand that there are many very small phase-waves.

<Quasi Lyapunov exponent>

Figure 4(d) shows QLE_{50}. We can observe that QLE asymptotically becomes to around -13.

5. Conclusion

We investigated behaviors of IERs and QLEs of when phase-inversion waves or phase-waves were propagating. One of differences between phase-inversion waves and phase-waves was clarified by using IERs. It was clarified that details of motion of phase-waves can be observed. The QLEs asymptotically became to about -13. In these results, we can say that it is effective approach to analyze phase-inversion waves and the phase-waves by using IERs and QLEs.

References

[1] L. Lin, F. Li and M. Ma, "Synchronization of bio-nanomachines nased on molecular diffusion," *IEEE Sensors Journal*, vol. 16, issue 16, pp. 7267-7277, 2016.

[2] M. Yamauchi, M. Wada, Y. Nishio and A. Ushida, "Wave propagation phenomena of phase states in oscillators coupled by inductors as a ladder," *IEICE Trans. Fundamentals*, vol. E82-A, no. 11, pp. 2592-2598, Nov. 1999.

[3] M, Yamauchi, Y. Nishio and A. Ushida, "Phase-waves in a ladder of oscillators," *IEICE Trans. Fundamentals*, vol. E86-A, no. 4, pp. 891-899, Apr. 2003.

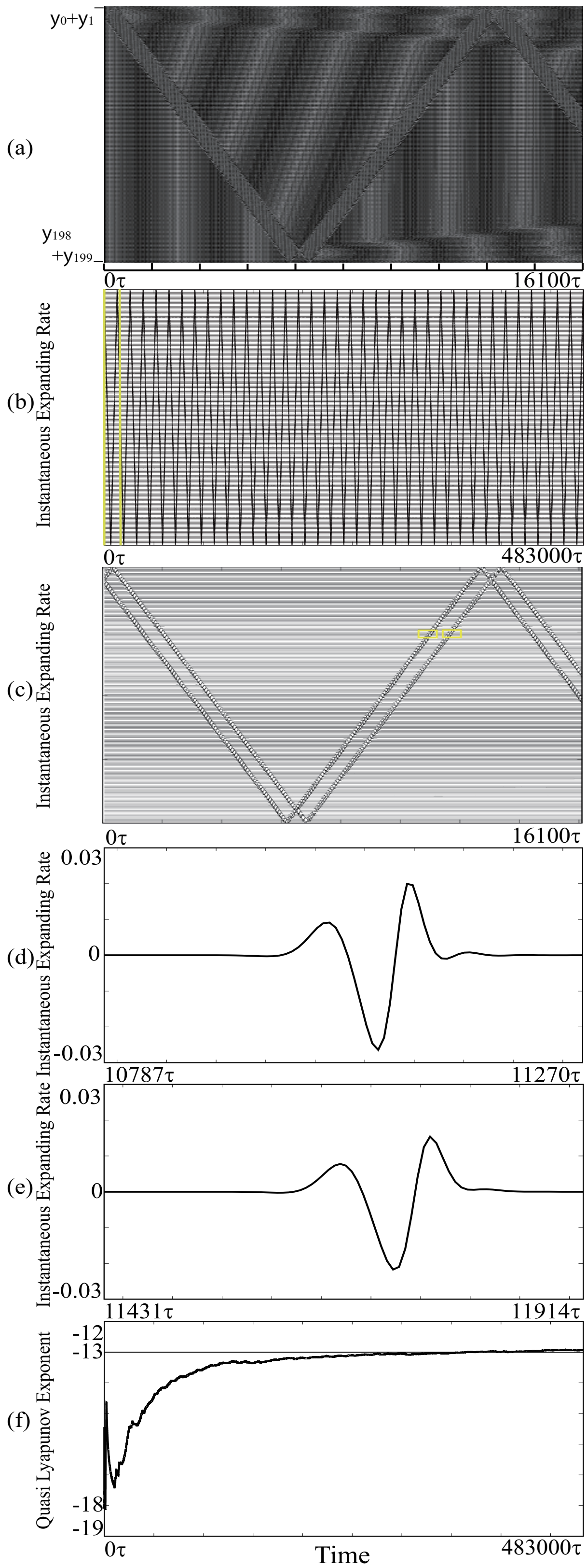

Figure 2: Wide-type phase-inversion waves. (a) phase states (0τ to 16100τ), (b) whole of IERs, (c) behavior of IER_{50}(0τ to 16100τ), (d) behavior of IER_{50}(10787τ to 11270τ), (e) behavior of IER_{50}(11431τ to 11914τ), (f) QLE_{50}.

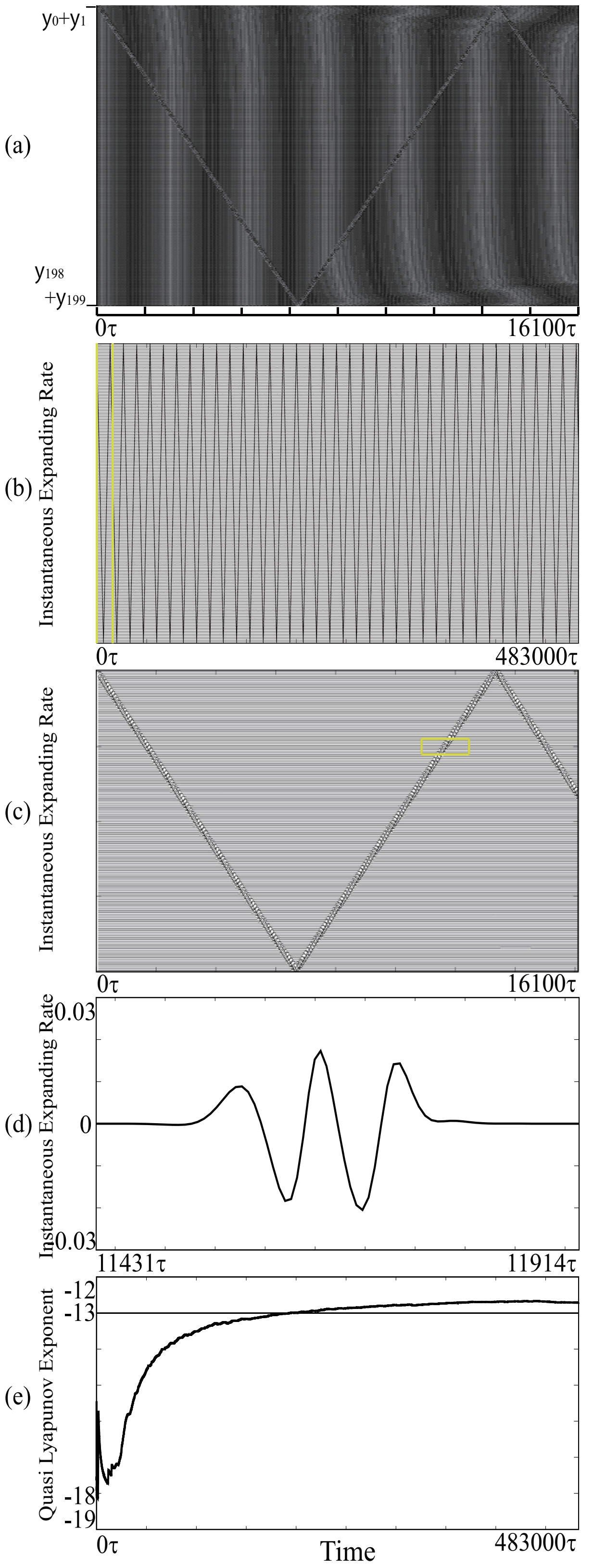

Figure 3: Thin-type phase-inversion waves. (a) phase states (0τ to 16100τ), (b) whole of *IER*s, (c) behavior of IER_{50}(0τ to 16100τ), (d) behavior of IER_{50}(11431τ to 11914τ), (e) QLE_{50}.

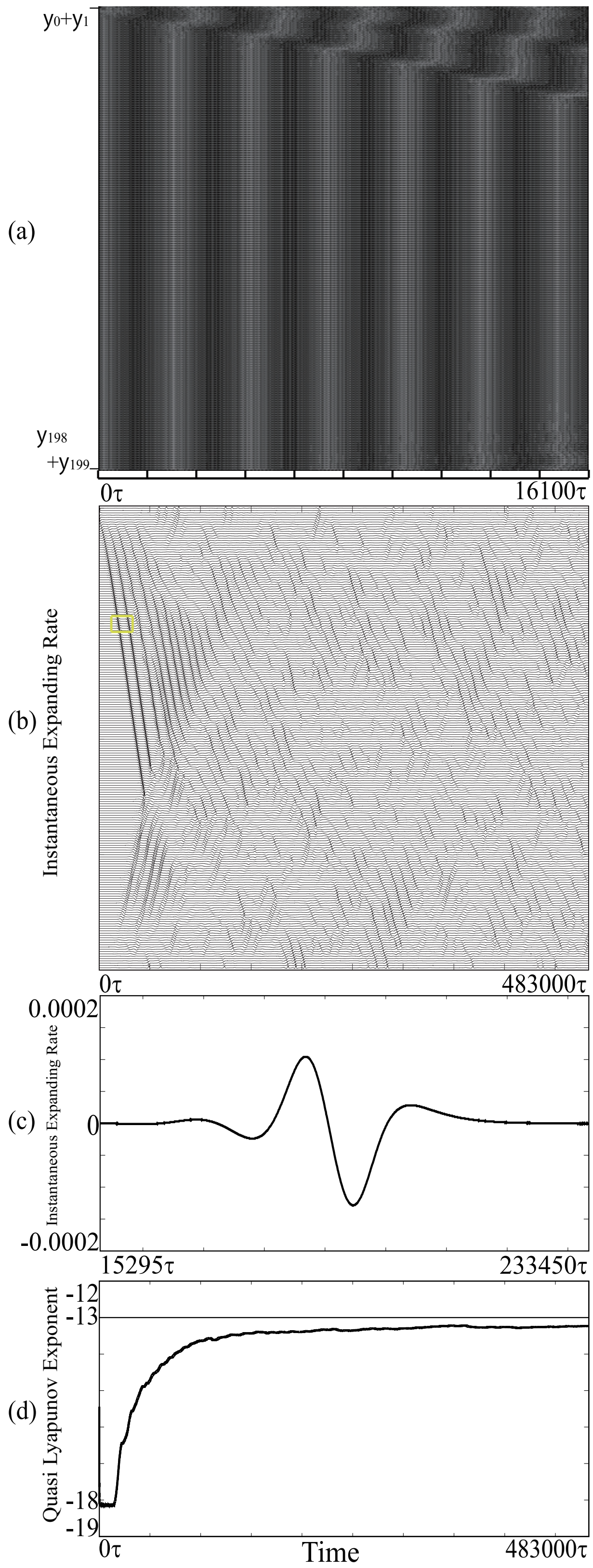

Figure 4: Phase-waves. (a) phase states (0τ to 16100τ), (b) whole of *IER*s, (c) behavior of IER_{50}(15295τ to 233450τ), (d) QLE_{50}.